

A nuclear microscopy study of trace elements Ca, Fe, Zn and Cu in atherosclerosis

F. Watt^{a,*}, R. Rajendran^{a,b}, M.Q. Ren^{a,b}, B.K.H. Tan^c, B. Halliwell^b

^a Centre for Ion Beam Applications, Department of Physics, National University of Singapore, Singapore 117542, Singapore

^b Department of Biochemistry, National University of Singapore, Singapore 117542, Singapore

^c Department of Pharmacology, National University of Singapore, Singapore 117542, Singapore

Available online 19 May 2006

Abstract

Quantitative mapping of trace elements Ca, Fe, Zn and Cu can be achieved in biological tissue using a nuclear microprobe. Presented here is a brief review of the work we have carried out in the last decade using the nuclear microscope to try and elucidate the role of trace elements Fe, Zn, Cu and Ca in induced atherosclerosis in New Zealand White rabbits fed on a 1% cholesterol diet. The lesions were studied using nuclear microscopy, incorporating a combination of ion beam techniques: particle induced X-ray emission (PIXE), Ruthenium backscattering spectrometry (RBS) and scanning transmission ion microscopy (STIM).

Iron is present in early lesions at concentrations around seven times higher than the artery wall. Measurements of localized lesion iron concentrations were observed to be highly correlated with the depth of the lesion in the artery wall for each individual animal, implying that local elevated concentrations may provide an accelerated process of atherosclerosis in specific regions of the artery. When the rabbits were kept mildly anaemic, thereby reducing iron levels in the lesion, the progression of the disease was significantly slowed. Iron chelation using desferal showed that early treatment (three weeks into the high fat diet) for relatively long periods (nine weeks) significantly retarded the progression of the disease. Zinc is depleted in the lesion and is also observed to be anti-correlated with local lesion development and feeding the rabbits on a high fat diet with zinc supplements inhibited lesion development, although since no significant increase in lesion zinc levels was measured, this anti-atherosclerotic effect may be indirect. Copper, measured at low levels (~3 ppm) in the early lesion, is also depleted compared to the artery wall, suggesting that it is not a major factor in atherogenesis. Calcium is also depleted in early lesions, although at a later stage mineral deposition (hydroxyapatite) is observed to take place in the lesion/artery wall interface (intima), and subsequently in the lesion.

These results are consistent with the hypotheses that iron plays a role in atherosclerosis probably through the production of free radicals and that zinc has an indirect protective effect. Copper appears to have a minor role due to its low lesion concentrations and hydroxyapatite deposition is a relatively late event.

© 2006 Published by Elsevier B.V.

PACS: 78.70.-g; 82.80.Yc; 87.64.-t

Keywords: Atherosclerosis; Elemental mapping; Nuclear microscopy; Nuclear microprobe; Iron; Zinc; Calcium; Copper

1. Introduction

Atherosclerosis is a disease of large and medium-sized arteries and is characterized by endothelial dysfunction (a malfunction of the cells lining the inside artery wall), vascu-

lar inflammation, the migration of smooth muscle cells to the inner lining of the artery (intima) and the buildup of lipids, cholesterol and cellular debris within the intima of the vessel wall. Oxidized low-density lipoproteins (oxLDL) produced by oxidative modifications of LDL in the sub-endothelial space have been demonstrated to be critically involved in atherogenesis through their intensive pro-inflammatory activity. Circulating monocytes infiltrate the intima of the vessel wall and the tissue macrophages

* Corresponding author. Tel.: +65 6872815; fax: +65 67776126.

E-mail address: phywattf@nus.edu.sg (F. Watt).

act as scavenger cells, taking up oxLDL and forming the characteristic foam cell of early atherosclerosis. These activated macrophages produce numerous factors that are injurious to the endothelium, leading to plaque formation. In later stages, calcification in the damaged region leads to hardening of the artery wall, coupled with acute and chronic arterial obstruction (see e.g., the review article [1]). The mechanisms of atherogenesis are not yet fully understood despite the intense study in this area over the last few decades.

The role of trace elements in the progression of atherosclerosis has in general not been widely studied because of the lack of analytical techniques that can both map and accurately quantify these trace elements in atherosclerotic tissue down to the cellular level. Iron has been implicated in the oxidative modification of LDL through the catalysis of free radical reactions [2,3] and copper has similarly been implicated through a similar pro-oxidant role [4]. Calcium is now considered a relatively late event in the progression of the disease [5–7] with the calcification process resembling the formation of bone (hydroxyapatite) appearing in the region between the atherosclerotic lesion and the smooth muscle wall of the artery. Zinc may play a role in slowing down the progression of the disease, perhaps through its anti-inflammatory properties and its ability to suppress the proliferation of the smooth muscle cells adding to intimal thickening. Zinc is also believed to have specific anti-atherogenic properties by inhibiting oxidative stress-responsive transcription factors that are activated during an inflammatory response in atherosclerosis [8,9].

Nuclear microscopy [10], a technique based on a focused beam of MeV nuclear particles (usually protons), has the ability to image the morphology of the tissue and map the trace elements Fe, Ca, Zn and Cu using a combination of three simultaneously applied ion beam techniques. Scanning transmission ion microscopy (STIM) is a technique used to investigate samples which are thin enough for transmission of a MeV proton beam. For relatively thin organic samples (30 μm or less), essentially all incident protons that have not suffered nuclear backscattering collisions will pass through the sample. Measurement of the energy loss of the transmitted proton provides a morphological image (through density variations) of the sample. Particle induced X-ray emission (PIXE) is now a well established technique for trace elemental analysis offering non-destructive multi-elemental capability and low detection limits. It allows simultaneous detection of multiple elements, with high quantitative accuracy coupled with an analytical sensitivity down to 1 ppm in biological material such as tissue sections and cells. Rutherford backscattering spectrometry (RBS) relies on the energy measurement of protons that have backscattered from atomic nuclei in the sample and provides information on the accumulated proton charge for each analysis, matrix composition and thickness of the tissue (i.e. carbon, oxygen, etc.). The combination of PIXE and RBS therefore allows quantitative measurements of elemental concentration.

This paper is a review of the work on the role of trace elements in atherosclerosis carried out over the last decade at the Centre for Ion Beam Applications (formerly the Research Centre for Nuclear Microscopy), Department of Physics, National University of Singapore.

2. Materials and Methods

2.1. Nuclear microscopy

The nuclear microscopy measurements were carried out at the NUS Centre for Ion Beam Applications (CIBA) using a 2.1 MeV proton beam focused to a 1- μm spot size [11]. A HVEE ‘Singletron’ accelerator provided the proton beam and the beam was focused to typical operating proton beam sizes of 1 μm at beam currents of around 300–400 pA using an Oxford Microbeams OM2000 focusing system. PIXE data, backscattered protons (RBS) and protons scattered forward at 15° to the incoming beam (off-axis STIM) were recorded simultaneously using the OMDAQ data acquisition system [12], both on-line and in list-mode. List mode files were later replayed off-line and elemental concentrations from selected areas of the target were calculated using the computer code GUPIX [13] by normalizing PIXE data to the irradiated mass and charge obtained from the corresponding RBS spectra. The energy of the proton beam, at 2.1 MeV, was chosen to avoid a strong carbon nuclear elastic resonance at 1.7 MeV which would otherwise have distorted the RBS spectrum. The setup was optimized for the analysis of iron, copper, calcium and zinc in biological samples, with a 300 μm perspex ‘magic’ filter with a central 1 mm hole [11] coupled with a Gresham 80 mm² Si(Li) X-ray detector. The target was orientated at 45° to the incoming beam and the Si(Li) detector orientated 90° to the beam axis. In this geometry the detector crystal can be positioned as close as 16 mm from the target, thereby maximising X-ray detection efficiency for trace elements.

2.2. Atherosclerosis samples

The atherosclerosis models used were New Zealand white male rabbits obtained from the Laboratory Animal Centre (Sembawang, Singapore). *Normal control rabbits* were rabbits fed on a normal chow diet. *HFD control rabbits* were fed on a normal chow supplemented with a high fat diet HFD SF00-221 (Modified GPR + 1% Cholesterol). Both these diets were supplied by Glen Forrest Stockfeeders, Western Australia. *Test rabbits* were fed the high fat diet but also subjected to a series of tests from iron chelation to zinc supplements (further details given below). The animals were sacrificed with *i/v* injection of Hypnorm (0.3 ml/kg) in accordance with guidelines approved by the NUS local Animal Care and Use committee. The aortic arch was removed and cut into three segments A, B and C. Each segment was quickly flushed (inside and out) with de-ionized water to remove blood residuals and quickly

embedded with “Thermo Shandon” (M-1 embedding matrix for frozen sectioning), making sure that the lumen was filled with matrix to maintain the physical integrity of the artery section during subsequent cryo-sectioning. The samples were quickly flash frozen in liquid nitrogen and stored at -85°C for later sectioning and analysis. From the frozen blocks, sections of $15\ \mu\text{m}$ were cut using a Leica CM3050S cryostat and picked up on freshly made $0.5\ \mu\text{m}$ pioloform film supported on nuclear microscopy holders. The pioloform film is self supporting and strong enough to support the tissue, free from trace metals and can withstand focused proton beams. Serial sections of $25\ \mu\text{m}$ thickness were also cut and picked up on gelatin coated slides for H and E (Hematoxylin and Eosin) staining. These sections were used for lesion area analysis, carried out using a Carl Zeiss Axiophot 2 image analyzer utilizing the KS400 (version 3.18) analysis software. Stained sections were not used for nuclear microscopy analysis, since the use of stains and fixative agents undermine the integrity of the sample elemental composition. In our work, Student *t*-tests were used in order to ascertain the significance of test and control comparisons, with $p = 0.05$ considered as the boundary between significance and non-significance.

3. Results and discussion

3.1. Elemental composition of early lesions

Normal control rabbits fed on a normal diet did not exhibit atherosclerotic lesions, whereas HFD control rabbits (high fat diet – 1% cholesterol) animals exhibited atherosclerotic lesion formation starting at around 4–6 weeks. Fig. 1 shows the results from a typical nuclear microscopy scan taken from a rabbit eight weeks on the high fat diet. The STIM image indicates that the density and morphology of the lesion is very different compared with the smooth muscle cells in the artery wall and in this particular sample it is noticeable that the lesion is not uniformly developed around the artery wall. The phosphorus results show that P is elevated in the lesion from around 3200 to 5600 ppm (parts per million dry weight) presumably due to the increased presence of phospholipids. The phosphorus map therefore also acts as an indicator for the spatial extent of the lesion and can be used together with the STIM image as a confirmation of the lesion boundary. The iron map indicates that iron levels are elevated in the lesion and previous results [14] have shown that iron concentrations in the lesion (90 ppm) on average are higher compared with the artery wall (12 ppm). Copper levels in general are much lower and nearer the levels of detection for PIXE, but longer scans (up to 4 h with a beam current of 1 nA) showed a depletion in the lesion (~ 3 ppm) compared with the smooth muscle cells in the artery walls (~ 6 ppm) (see Fig. 2(c)). Zinc also showed a depletion in the lesion (~ 50 ppm) compared with the artery walls (~ 100 ppm). The lesion in Fig. 1 indicates a high level of

calcium mineralisation within the lesion and interface. Interestingly, we have also observed that in some developed lesions, where calcification had not yet taken place (see Fig. 2(b) and (d)), calcium concentrations were depleted (~ 450 ppm) compared with the adjacent healthy wall (~ 575 ppm).

3.2. Iron

In 1981, Sullivan [15] suggested that premenopausal women suffered a lower incidence of coronary heart disease compared with men of the same age because of their lower body iron storage. Any unregulated iron (Fe^{2+}) has the potential to catalyze and generate hydroxyl radicals (OH) from superoxide and hydrogen peroxide via the Fenton reaction [16]. The highly reactive hydroxyl radicals subsequently cause lipid peroxidation, degradation of other macromolecules, leading to cell damage or death. Several epidemiologic studies have investigated the role of iron as a potential risk factor in coronary heart disease [17–23], although many of these types of studies have conflicting conclusions.

Our nuclear microscopy investigations on early lesions (see Fig. 1) show that iron is substantially increased in the lesion. Although nuclear microscopy cannot give information on the chemical nature or state of the Fe, experiments by us have indicated that inducing mild anaemia decreases the progression of atherosclerosis in cholesterol-fed rabbits, in conjunction with decreased lesion iron content [24]. In a similar study using apo E-deficient mice, vascular iron deposition was shown to be closely related to progression of atherosclerosis and LDL oxidation [25]. In this study, the extent of atherosclerosis in the mice were found to be significantly lower in mice fed a low-iron diet compared to control animals.

We have also investigated the use of the iron chelator, *desferal*, which forms a stable complex with ferric iron thereby decreasing its availability for the production of reactive oxygen species and resultant free radical damage. Desferal has been found to protect against tissue damage in vivo, in several model systems, probably through its ability to inhibit iron-dependent free radical reactions [26]. We have observed that for rabbits fed with a high fat diet, desferal induced iron chelation applied six weeks into the cholesterol diet for a period of two weeks does not slow the lesion development, but when applied for a longer period of four weeks indicates a possible trend ($p = 0.07$) to the reduction of lesion progression [27]. In a more recent follow-up study [28], rabbits were fed with the high fat diet for either eight weeks (with the last five weeks injected daily with desferal), or for 12 weeks (with the last nine weeks injected with desferal). A significant reduction in average lesion area ($p = 0.038$) was observed in the 12-week treated test animals as compared with 12-week HFD controls. The average lesion iron level of the 12 week treated animals (58 ppm dry weight) was significantly lower ($p = 0.030$) than in 12-week control animals (95 ppm dry weight). Dur-

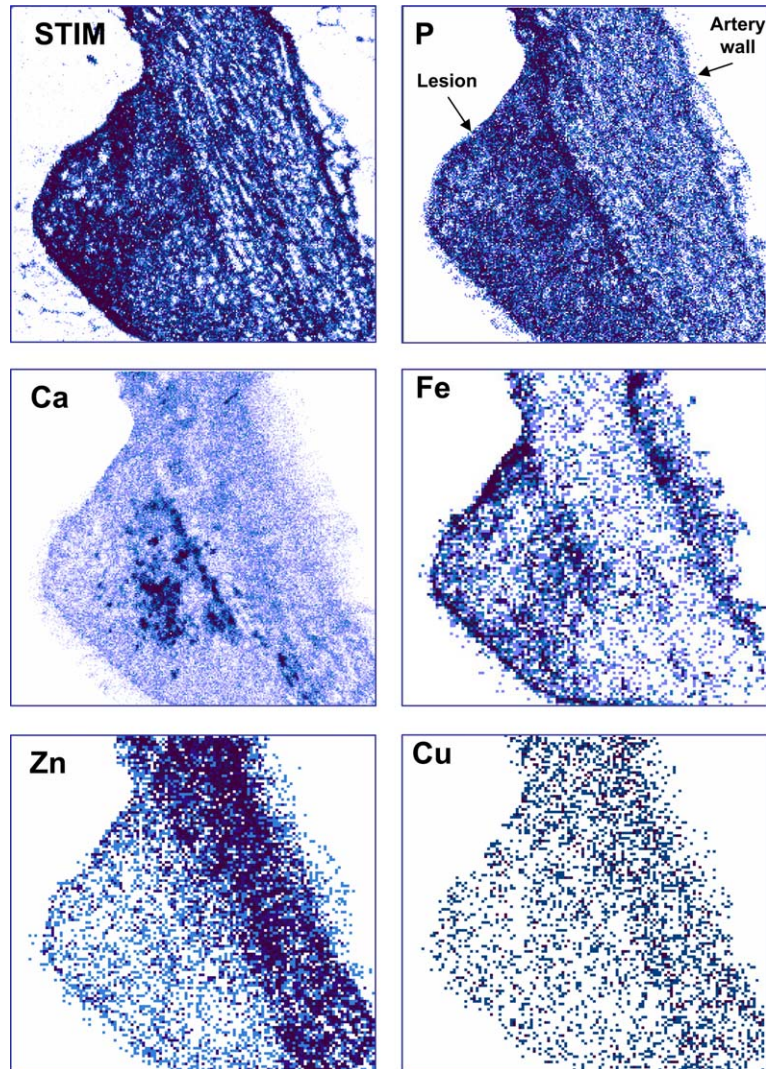


Fig. 1. STIM image and elemental maps of an early lesion (New Zealand white rabbit fed for eight weeks on a high fat diet (1% cholesterol)). In this example, the lesion is not uniform around the artery wall, but protrudes from the artery wall. The lesion is delineated by the STIM images (higher density) and P maps (enhanced P). The scan size is $1200 \times 1200 \mu\text{m}$.

ing our investigations we have also noticed that the extent (depth) of the atherosclerotic lesions varied both along the length of the artery and also around the artery cross-section for each individual rabbit. Measurements of localized iron concentrations were highly correlated with the depth of the lesion in the artery wall for each individual animal, implying that local elevated concentrations of iron present in early lesions may provide an accelerated process of atherogenesis in specific regions of the artery wall [27].

3.3. Zinc

Zinc is a cofactor of many enzymes and has been shown to have anti-inflammatory and anti-proliferatory properties. Recent work has shown that zinc can reduce the effects of carotid artery injury induced in rats by balloon dilatation, by reducing smooth muscle cell proliferation and intimal thickening [9]. Studies also indicate that zinc is vital to

vascular endothelial cell integrity and zinc deficiency causes severe impairment of the endothelial barrier function [8,29–32]. Zinc is believed to have specific anti-atherogenic properties by inhibiting oxidative stress-responsive transcription factors that are activated during an inflammatory response in atherosclerosis.

Our nuclear microscopy investigations on early lesions (see Fig. 1) show that zinc is substantially depleted in the lesion compared with the adjacent artery wall. Our investigations have also shown that localized lesion zinc concentrations are inversely correlated with lesion depth [27]. In more recent work [33] we investigated the effect of zinc supplements on the progression of atherosclerotic lesion growth. Test rabbits received a high cholesterol diet with Zn supplements (diet SF03-017-modified GPR + 1% Cholesterol + 1000 ppm (1 g/kg) zinc as zinc carbonate) for eight weeks and control rabbits were fed only with a high cholesterol diet for the same period of time. Lesion area

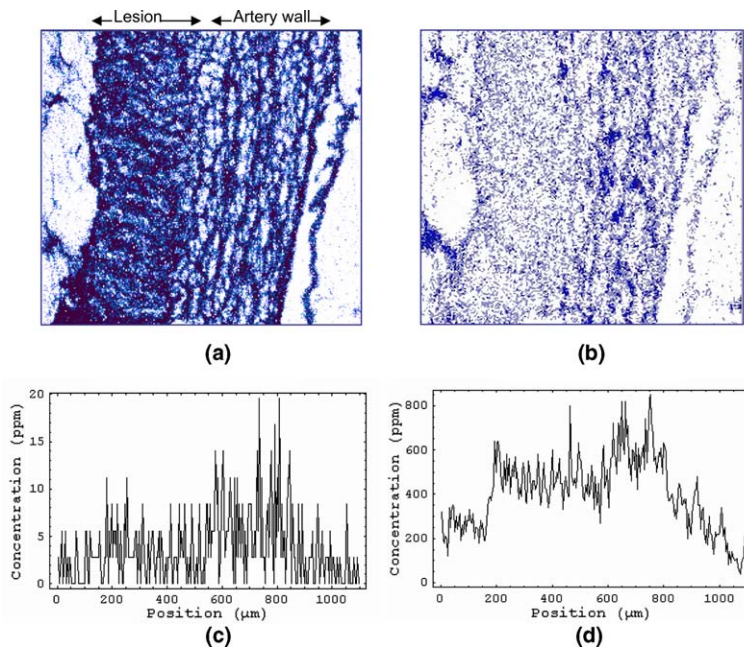


Fig. 2. (a) STIM image and (b) calcium elemental map of an early lesion (New Zealand white rabbit fed for eight weeks on a high fat diet (1% cholesterol)). In this example, the lesion has developed relatively uniformly around the artery wall and shows minimal calcification. The scan size is 1100×1100 microns. (c) A line scan of the copper concentrations and (d) the calcium concentrations, across the lesion + artery, depicted in (a) showing a depletion in both Ca and Cu in the lesion.

analyses using light microscopy showed that the average lesion area was significantly reduced ($P = 0.0045$) for the rabbits on the zinc supplement diet (with average lesion areas of 1.0 mm^2 for the zinc test models compared with 3.0 mm^2 for the HFD control group models). However, elemental analysis of the lesion and adjacent artery wall showed that the average zinc level remained the same for both the lesion and the artery wall for both test and control models, whilst the iron levels are reduced from 43 ppm to 31 ppm (in the lesion) and from 17 ppm to 6 ppm (in the artery wall). This raises the possibility that zinc may act as an endogenous protective factor against atherosclerosis by reducing iron levels.

3.4. Copper

Unregulated copper is highly pro-oxidative, since it can catalyse free radical formation. However, it also can be anti-oxidative through its role in copper/zinc superoxide dismutase [34]. Stadler [35] using ICPMS (inductively coupled plasma mass spectrometry), has recently reported that statistically elevated levels of iron and copper were detected in the intima of lesions compared with healthy controls (ex vivo). The work of Lamb et al. [36] has shown that dietary copper supplementation significantly *decreased* aortic atherosclerosis in cholesterol-fed rabbits. The lesions from animals that received the copper supplement contained fewer smooth muscle cells and fewer apoptotic cells. Their data suggests that copper supplements inhibit the progression of atherogenesis, perhaps by reducing the migration of smooth muscle cells from the media to the intima. Alissa

et al. [37] have recently found that when New Zealand white rabbits are fed dietary supplements of copper or zinc separately in conjunction with a high fat diet, aortic atherogenesis was inhibited, although there was no significant additional effect when zinc and copper were given in combination. A recent study involving four European centers shows that dietary Cu supplements (up to 7 mg/day – at the extreme end of normal dietary intake) for humans have no adverse effects on LDL susceptibility to in vitro induced oxidation [38].

Our results using nuclear microscopy in the rabbit model (see for example Fig. 2(c)) show that copper is depleted in the early lesion, at an average level of ~ 3 ppm compared with ~ 6 ppm of adjacent artery wall. Compared with iron, which is enhanced in the lesion compared with artery wall at levels around 90 ppm, copper concentrations in the early lesion are a factor of 30 lower and therefore are unlikely to have the same impact as unregulated iron in catalysing free radicals or promoting copper mediated LDL oxidation. Our work therefore is consistent with the hypothesis that in the rabbit model, copper does not play an adverse role in the progression of the disease.

3.5. Calcium

Arterial calcification is a relatively late event in atherogenesis. However, because it can decrease elasticity and lead to rupture of the artery wall, a great deal of work has been carried out recently to try and elucidate the mechanisms of mineralization. Far from the mineralization pro-

cess being a passive deposition process, it is now recognised that arterial mineralisation is an active process involving complex bio-molecular mechanisms. There are two major types of calcification in arteries: calcification of the mid layer of the artery (media tunica) and calcification within subdomains of atherosclerotic plaque. Of particular interest are increasing parallels between cellular and molecular features of arterial calcification and bone biology [6]. By analogy with known bone biology, Doherty [5] has proposed a homeostatic mechanism wherein the two main cellular mediators are osteoblast-like cells and osteoclast-like cells (OLCs). He proposes that arterial mineral metabolism is normally in balance, but in pro-inflammatory plaque microenvironments, immune-modulating cytokines facilitate recruitment and development of osteoblast-like cells and OLCs, uncouple their activities and produce a net mineral deposition. In a study with New Zealand White rabbits fed on a high fat diet (1% cholesterol) for 3 and 6 months, Hsu et al. [39] investigated the calcification process using histochemical staining and revealed that after 6 months on the high fat diet, calcification appeared to occur predominantly in the intimal areas immediately adjacent to the media. Fourier transform imaging analysis demonstrated that the mineral deposited in atherosclerotic rabbit aortas was a hydroxyapatite-like phase and that production of calcifiable cavities (vesicles) preceded substantial calcification.

In the nuclear microscopy elemental maps presented in Fig. 1 the mineralisation process is relatively advanced, with large and fragmented co-localised deposits of Ca and P in both the lesion and the lesion artery interface. Individual measurements of the calcium and phosphorus content of the mineral deposits yielded values of the Ca/P ratios from 1.5 to 2.1, consistent with the mature deposits being composed of either calcium carbonate (Ca/P = 1.94) or hydroxyapatite (Ca/P = 2.15). However, in other results on early lesions where the calcification is not yet apparent, we have observed a slight depletion in calcium in the lesion compared with artery wall (450 ppm compared with 575 ppm) (see e.g., Fig. 2(d)).

4. Conclusion

In a series of investigations spanning over a decade we have used the nuclear microscope to try and elucidate the role of trace elements Fe, Zn, Cu and Ca in induced atherosclerosis in the rabbit model and the results to date can be summarized as follows: (A) *Iron*: Iron is present in early lesions at concentrations around seven times higher than the artery wall (~90 ppm compared with ~12 ppm). The extent (depth) of the atherosclerotic lesions varies both along the length of the artery and also around the artery cross-section for each individual rabbit. Measurements of localized lesion iron concentrations were highly correlated with the depth of the lesion in the artery wall for each individual animal, implying that local elevated concentrations may provide an accelerated process of atherogenesis in spe-

cific regions of the artery wall. When the rabbits were kept mildly anaemic, thereby reducing iron levels in the lesion, the progression of the disease was significantly slowed. Iron chelation using desferal yielded mixed results: Delayed desferal treatment over short periods (two weeks treatment after six weeks into the high fat diet) appeared to have little effect, but a significant effect was noticed when the treatment was both earlier (three weeks into the high fat diet) and longer (for nine weeks). These results are consistent with the theory that iron plays a role in angiogenesis, probably through the production of free radicals, and that by removing iron from the lesion the rate of progression of the disease is slowed. (B) *Zinc*: Unlike iron, zinc is depleted in the early lesion compared to the artery wall (~50 ppm compared with ~100 ppm) and has a concentration which is anti-correlated with localised lesion depth. Feeding the rabbits on a high fat diet with zinc supplements inhibited lesion development. However, this appears to be an indirect effect since no significant increase in lesion zinc levels were measured, raising the possibility that zinc may act as an endogenous protective factor against atherosclerosis, perhaps by reducing lesion iron levels. (C) *Copper*: Copper is observed in the lesions and the artery wall at the few parts per million level and is therefore at the limits of sensitivity of PIXE. Nevertheless, it is apparent from our studies that copper is depleted in the lesion compared to the artery wall (~3 ppm compared with ~6 ppm). Copper, like iron, can catalyse free radicals through the Fenton reaction, although because of its low lesion levels compared with iron (~30 times lower) we believe it unlikely to play a major role in atherogenesis. (D) *Calcium*: We have observed lesions (from rabbits fed for eight weeks on a high fat diet) where calcification is not apparent, in which there is a depletion of calcium in the lesion compared with the adjacent artery wall (450 ppm compared with 575 ppm). However, the mineralisation process is not consistent from rabbit to rabbit, with some lesions exhibiting calcification much later than others. We have also observed calcification in lesions (also from rabbits fed for eight weeks on a high fat diet) as co-localised calcium and phosphorus deposition (consistent with the elemental profile of hydroxyapatite). Our observations are that calcification is a relatively late event, where in general, mineral deposits occur first in the interface between the artery and the lesion, followed by deposition in the lesion.

The nuclear microscope has the unique capability of *quantitative* trace element mapping down to the parts per million level at spatial resolutions down to the sub-cellular level and these features make the technique ideally suited to the simultaneous measurements of trace elements in biological tissues.

Acknowledgements

We are grateful to the Faculty of Science, National University of Singapore for support through the grant R 144 000 021 112 and to the Office of Life Sciences, Singapore

Totalisator Board and Academic Research Fund of the National University of Singapore for the support grants R172 000 072 112/650/432.

References

- [1] A.C. Langheinrich, R.M. Bohle, *Virchows Archiv.* 446 (2) (2005) 101.
- [2] D. Steinberg, S. Parthasarathy, T.E. Carew, J.C. Khoo, J.L. Witztum, *N. Engl. J. Med.* 320 (14) (1989) 915.
- [3] H. Lum, K.A. Roebuck, *Am. J. Physiol. (Cell Physiol.)* 280 (2001) C719.
- [4] S.M. Lynch, B. Frei, *J. Lipid Res.* 34 (10) (1993) 1745.
- [5] T.M. Doherty, K. Asotra, L.A. Fitzpatrick, J.-H. Qiao, D.J. Wilkin, R.C. Detrano, C.R. Dunstan, P.K. Shah, T.B. Rajavashisth, *PNAS* 100.20 (2003) 11201.
- [6] T.M. Doherty, L.A. Fitzpatrick, D. Inoue, J.-H. Qiao, M.C. Fishbein, R.C. Detrano, P.K. Shah, T.B. Rajavashisth, *Endocrine Rev.* 25 (2004) 629.
- [7] H.H.T. Hsu, O. Tawfik, F. Sun, *Cardiovascular Pathol.* 13 (2004) 3.
- [8] G. Reiterer, M. Toborek, B. Hennig, *J. Nutr.* 134 (7) (2004) 1711.
- [9] M. Berger, E. Rubinraut, I. Barshack, A. Roth, G. Keren, J. George, *Atherosclerosis* 175 (2) (2004) 229.
- [10] F. Watt, G.W. Grime, in: S.A.E. Johansson, J.L. Campbell, K.G. Malmqvist (Eds.), *Particle induced X-ray emission spectroscopy (PIXE)*, Chem. Anal., 133, John Wiley & Son Inc., 1995, p. 101.
- [11] F. Watt, I. Orlic, K.K. Loh, C.H. Sow, P. Thong, S.C. Liew, T. Osipowicz, T.F. Choo, S.M. Tang, *Nucl. Instr. and Meth. B* 85 (1994) 708.
- [12] G.W. Grime, M. Dawson, *Nucl. Instr. and Meth. B* 89 (1994) 223.
- [13] J.A. Maxwell, J.L. Campbell, W.J. Teesdale, *Nucl. Instr. and Meth. B* 43 (1989) 218.
- [14] P.S.P. Thong, M. Selley, F. Watt, *Cellular Molecular Biol.* 42 (1) (1996) 103.
- [15] J.L. Sullivan, *Lancet* 1 (1981) 1293.
- [16] C. Rice-Evans, R. Burdon, *Prog. Lipid Res.* 32 (1993) 71.
- [17] J.T. Salonen, K. Nyyssonen, H. Korpela, J. Tuomilehto, R. Seppanen, R. Salonen, *Circulation* 86 (1992) 803.
- [18] M.K. Magnusson, G. Thorgeirsson, *Circulation* 89 (1994) 102.
- [19] T.P. Tuomainen, R. Salonen, K. Nyyssonen, J.T. Salonen, *BMJ* 314 (1997) 793.
- [20] D.M. Baer, I.S. Tekawa, L.B. Hurley, *Circulation* 89 (1994) 2915.
- [21] C.T. Sempos, A.C. Looker, R.F. Gillum, *N. Engl. J. Med.* 330 (1994) 1119.
- [22] Y. Liao, R.S. Cooper, D.L. McGee, *Am. J. Epidermiol.* 139 (1994) 704.
- [23] A. Ascherio, W.C. Willett, E.B. Rimm, E.L. Giovannucci, M.J. Stampfer, *Circulation* 89 (1994) 969.
- [24] D. Ponraj, J. Makjanic, P.S.P. Thong, B.K.H. Tan, F. Watt, *FEBS Lett.* 459 (1999) 218.
- [25] T.S. Lee, M.S. Shiao, C.C. Pan, *Circulation* 99 (1999) 1222.
- [26] B. Halliwell, *Free Radic. Biol. Med.* 7 (1989) 645.
- [27] R. Minqin, F. Watt, B.T.K. Huat, B. Halliwell, *Free Radic. Biol. Med.* 34 (6) (2003) 746.
- [28] R. Minqin, R. Rajendran, N. Pan, B.K.H. Tan, W.-Y. Ong, F. Watt, B. Halliwell, *Free Radic. Biol. Med.* 38 (9) (2005) 1206.
- [29] B. Hennig, Y. Wang, S. Ramasamy, C.J. McClain, *J. Nutr.* 122 (1992) 1242.
- [30] J. Clair, R. Talwalkar, C.J. McClain, B. Hennig, *J. Trace Elements Exp. Med.* 7 (1995) 143.
- [31] C. McClain, P. Morris, B. Hennig, *Nutrition* 11 (Suppl. 1) (1995) 117.
- [32] J.H. Beattie, I.S. Kwun, *Br. J. Nutr.* 91 (2) (2004) 177.
- [33] M.Q. Ren, R. Rajendran, N. Pan, B.T.K. Huat, B. Halliwell, F. Watt, *Nucl. Instr. and Meth. B* 231 (2005) 251.
- [34] B. Halliwell, J.M.C. Gutteridge, *Free Radicals in Biology and Medicine*, fourth ed., Oxford University Press, 2006.
- [35] N. Stadler, R.A. Lindner, M.J. Davies, *Arteriosclerosis Thrombosis Vascular Biol.* 24 (5) (2004) 949.
- [36] D.J. Lamb, G.L. Reeves, A. Taylor, G.A.A. Ferns, *Atherosclerosis* 146 (1) (1999) 33.
- [37] E.M. Alissa, S.M. Bahijri, D.J. Lamb, G.A.A. Ferns, *Int. J. Exp. Pathol.* 85 (5) (2004) 265.
- [38] E. Turley, A. McKeown, M.P. Bonham, et al., *Free Radical Biol. Med.* 29 (11) (2000) 1129.
- [39] H.H.T. Hsu, N.C. Camacho, O. Tawfik, F. Sun, *Atherosclerosis* 161 (2002) 85.